Integrated analysis on m6A-related prognostic lncRNA signatures associated with prognosis and tumor immunotherapy in renal papillary cell carcinoma

Xinglong Dai (834511377@qq.com)
The First Affiliated Hospital of Chongqing Medical University
Menghua Zeng
The First Affiliated Hospital of Chongqing Medical University
Zhen Huang
The First Affiliated Hospital of Chongqing Medical University
Jun Zhang
The First Affiliated Hospital of Chongqing Medical University
Zhengqiang Wei
The First Affiliated Hospital of Chongqing Medical University
Ziwei Wang
The First Affiliated Hospital of Chongqing Medical University

Research Article

Keywords: Kidney renal papillary cell carcinoma, M6A, LncRNA, Prognosis, Tumor immuneotherpay

Posted Date: April 15th, 2022

DOI: https://doi.org/10.21203/rs.3.rs-1548461/v1

Abstract

Background

To elucidate the prognostic patterns of m6A-related lncRNAs and construct a prognostic model of m6A-related lncRNAs in Kidney renal papillary cell carcinoma (KIRP).

Methods

We downloaded KIRP-related RNA-seq and clinical data from the TCGA dataset. Potential m6A-related prognostic lncRNAs in KIRP patients were selected by Pearson correlation test and univariate Cox analysis. KIRP patients were divided into two clusters using consensus clustering. The prognostic model of m6A-related lncRNAs was constructed to explore the relationship between m6A-related lncRNAs and clinical features and survival data using LASSO regression analysis. We also determined the relationship of risk models to tumor microenvironment (TME) and drug sensitivity.

Results

We first identified two m6A-related lncRNA pattern clusters by consensus clustering based on 32 m6A-related prognostic lncRNAs. Patients from cluster 2 were dramatically associated with poor prognosis, worse clinical grades, etc. Cluster 2 not only had higher immuneScore, ESTIMATEScore, and stromalScore but was also associated with higher levels of immune cell infiltration and expression of immune checkpoint molecules. Then, 14 m6A-related prognostic lncRNAs were selected and validated as independent and robust predictors of KIRP prognosis. Two nomograms based on age, tumor grade, clinical stage, and m6A-related lncRNAs expression were generated, showing high accuracy and reliability in predicting overall survival in KIRP patients. KIRP patients in the high-risk group had higher pN stage, pT stage, pM stage, advanced clinical stage, and higher tumor grade than the low-risk group. Importantly, cluster 2 with worse overall survival had a higher risk score than cluster 1, thus indicating consistency between the two methods for predicting survival in KIRP. Furthermore, some tumor-infiltrating immune cells, immune checkpoint molecules, and drugs sensitivity were closely related to the risk score of the prognostic model in KIRP patients.

Conclusion

We not only established a model of novel m6A-related prognostic lncRNAs with favorable prognostic value in KIRP patients, but also could provide new insights into tumorigenesis and predict treatment response in KIRP patients.

Background

Renal cell carcinoma (RCC) has become the third most common malignant tumor of the urinary system, with approximately 270,000 new cases and 116,000 deaths worldwide [1]. The pathological type of renal papillary cell carcinoma (KIRP) is different from Kidney renal clear cell carcinoma (KIRC), and its tumor cells are papillary or tubular structures, accounting for 7%-14% of renal cancer. With the development of medical imaging, the detection rate of early-stage renal cancer has gradually increased, and localized renal cancer can obtain satisfactory curative effects after radical nephrectomy or nephron-sparing renal tumor resection. With the rise of targeted therapy and new immunotherapy drugs, the efficacy and prognosis of advanced renal cancer have gradually improved. However, patients with advanced KIRP are prone to recurrence and metastasis after surgery, and treatment provides limited therapeutic benefit to only a small subset of patients. One of the common factors that accelerate the occurrence and development of KIRP is the accumulation of epigenetic changes [2]. Thus, elucidating the molecular mechanisms of KIRP and identifying potential molecular targets are necessary for developing new therapeutic agents and predicting the survival in patients with KIRP.

Aberrant N6-methyladenosine (m6A) modifications can generate aberrant splicing, instability, cancer stem cell self-renewal, and eccentric translation contributing to tumorigenesis and progression [3–5]. Dynamic m6A modifications are typically regulated by methyltransferase complexes (m6A 'writers'), demethylases (m6A 'erasers'), and signaling sensors (m6A 'readers'), respectively. The aberrant expression of long non-coding RNAs (lncRNAs) is near related to the malignancy of tumors, including tumor proliferation, apoptosis, drug resistance, and metastasis. However, m6A regulators in the dysregulation of lncRNAs in cancer development remain unclear, and whether m6A modification-related lncRNAs could be involved in the progression of KIRP remained to be elucidated. For example, m6A methyltransferase-like 3 (METTL3)-induced lncRNA ABHD11-AS1 was upregulated in non-small cell lung cancer (NSCLC), and its ectopic expression was closely related to the poor prognosis in patients with NSCLC [6]. METTL14-mediated Lnc-LSG1 m6A modification inhibited clear cell renal cell carcinoma metastasis by regulating ESRP2 ubiquitination [7]. Sun et al. found that a prognostic risk signature was constructed by the m6A methylation genes IGF2BP3, KIAA1429, and HNRNPC that accurately predicted survival outcomes in KIRP patients [8]. Therefore, the construction of m6A methylation-related lncRNAs and the identification of prognostic biomarkers in these lncRNAs are of great significance for understanding the mechanisms by which lncRNAs affect the prognosis of patients with KIRP. In our study, we performed a comprehensive KIRP RNA-seq and clinical data analysis using the TCGA database to establish an m6A-related lncRNA prognostic signature to predict the prognosis of KIRP patients.

Recently, immunotherapy and tyrosine kinase inhibitors (TKIs) have gradually been recognized as indispensable methods for the treatment of patients with renal cancer. Immune checkpoint blocker therapy was considered specialized anti-tumor immunotherapy targeting immune checkpoint proteins, including PD-L1, CTLA-4, LAG3, etc. Immune checkpoint proteins were associated with the tumor microenvironment (TME) that could be manipulated by tumor cells to regulate immune signaling pathways to evade immune responses and facilitate tumor development. Previous studies have shown that lncRNAs played a non-negligible role in cancer immunity [9–10], but the potential tumor immune mechanisms of m6A-related lncRNAs in KIRP remain unclear. This study aimed to analyze the correlation

of m6A-related lncRNA signature with the TME in KIRP and to explore the feasibility of tumor therapy from the mechanism of m6A-related lncRNAs.

Results

Identification of m6A-related prognostic lncRNAs in KIRP

The 289 tumor samples and 32 normal tissues from KIRP patients were obtained and downloaded from the TCGA database and rearranged. After identifying 14086 lncRNAs in the TCGA-KIRP dataset, we extracted the expression profiles of 23 m6A-methylation regulators in the TCGA-KIRP dataset and then evaluated the relationship between the 23 m6A methylation regulators and 14086 lncRNAs. LncRNAs associated with one or more of the 23 m6A methylation regulators (|Pearson R| > 0.3 and $p < 0.001$) were defined as m6A-related lncRNAs, and the results showed that 1387 m6A-related lncRNAs were discerned as m6A-related lncRNAs. The co-expression networks of 23 m6A methylation regulators and lncRNAs were drawn using the Cytoscape software 3.7.0 and shown in **Figure 1A**. Univariate Cox regression analysis was performed to analyze m6A-related prognostic lncRNAs with a p-value of 0.001. The results showed that 32 m6A-related lncRNAs were associated with the overall prognosis of KIRP patients (**Figure 1B and Table 1**). Differences between tumor and normal tissues in 32 m6A-related prognostic lncRNAs were analyzed and displayed as a heatmap (**Figure 1C**). The correlation of 32 m6A methylation regulators and m6A-related lncRNAs were plotted using the Sankey diagram in **Figure 1D**. Furthermore, the expression levels of 32 m6A-related prognostic lncRNAs differed in KIRP tissues and normal tissues (**Figure 1E**).

Consensus clustering of m6A-related lncRNAs determined in KIRP

Consensus clustering was used to classify KIRP patients into subgroups based on the similarities shown by the expression of m6A-related lncRNAs. K= 2 showed the least overlap and the best cluster stability from k= 2 to 9, with the lowest CDF values; thus, lncRNAs were classified into cluster 1 and cluster 2 (**Figures 2A-2C**). To further evaluate the prognostic value of m6A-related lncRNAs based on the lncRNAs subtype survival analysis, the overall survival of KIRP patients in cluster 2 was lower than that in cluster 1 (p= 0.011, **Figure 2D**). Heatmap showed the differences in m6A-related prognostic lncRNAs expression in the two clusters and their relationship to clinicopathological parameters. M6A-related prognostic lncRNAs in cluster 2 were markedly associated with advanced pN stage, pM stage, pT stage, clinical stage, and grade in KIRP patients, and these lncRNAs were independent of age and gender (**Figure 2E**). Therefore, these consensus clustering results showed a significant correlation between m6A-related lncRNAs and the prognosis of KIRP patients.

Correlation analysis of m6A-related lncRNAs with the TME and immune cell infiltration

To investigate the role of m6A-related prognostic lncRNAs in the KIRP immune microenvironment, we first analyzed the differences in immuneScore and immune cell infiltration and exhibited a vioplot between cluster 1 and cluster 2 (**Figure 3A**). Immune cells such as memory B cells, resting CD4

memory T cells and resting mast cells were highly aggregated in cluster 1 ($p< 0.05$). In contrast, naive memory B cells, T cell CD8, activated CD4 memory T cells, follicular helper T cells, and macrophages M1 were highly clustered in cluster 2 ($p< 0.05$). The average immuneScore, stromalScore, and ESTIMATEScore in cluster 2 were significantly higher than in cluster 1 (**Figures 3B-3D,** all $p< 0.01$). Next, we examined the mRNA levels of immune checkpoints in each cluster and their association with m6A-related prognostic lncRNAs. The expression levels of PD-L1, HAVCR2, LAG3, PDCD1LG2, SIGLEC15, and TIGIT were prominently higher in cluster 2 than in cluster 1 (**Figures 3E-3J**). Furthermore, the expression of CTLA4, TIGIT, and SIGLEC15 was considerably elevated in KIRP tissues compared with normal tissues (**Figure 3K**). Interestingly, PD-L1, HAVCR2, LAG3, SIGLEC15, and TIGIT were negatively correlated with multiple m6A-related prognostic lncRNAs, and only PDCD1LG2 was positively correlated with the expression of some m6A-related lncRNAs (**Figure 3L**).

Construction and validation of the m6A-related prognostic lncRNAs signature

To further identify the most potent prognostic signatures, we performed a LASSO Cox regression analysis to screen and integrate 14 m6A-related prognostic lncRNAs to predict overall survival in KIRP patients (**Figures 4A-4C**). The 289 KIRP patients were randomly divided into training cohorts and test cohorts, and then the risk scores were calculated for each KIRP patient and divided into high-risk and low-risk groups. Survival curves revealed that the high-risk group of KIRP patients had a worse prognosis than those of the low-risk group in both the training cohort (**Figure 4D,** $p < 0.001$) and the test cohort (**Figure 4G,** $p = 0.025$). To assess the accuracy of the model in predicting survival in KIRP patients, the ROC results showed a curve (AUC) of 0.929, 0.921, and 0.930 for 1-, 2-, and 3-year overall survival rates, respectively, in the training cohort (**Figure 4E**). ROC curves also showed that m6A-related prognostic lncRNAs accurately predicted overall survival in the test cohort, with AUCs of 0.759, 0.766, and 0.754 for 1-, 2-, and 3-year overall survival rates, respectively (**Figure 4H**). The ROC curve and concordance index indicated that m6A-related prognostic lncRNAs were promising for predicting overall survival in KIRP patients. Subsequently, we achieved a risk curve and assessed the survival status and risk of m6A-related lncRNAs based on this curve. These features consisted of 14 m6A-related prognostic lncRNAs with excellent distinguishing performance in predicting the prognosis of KIRP patients. As risk scores increased, the number of deaths and the high-risk ratios enhanced. In addition, the expression of protective lncRNAs (ZKSCAN7-AS1, DSG2-AS1, AL133355.1, AC135050.6 and ADAMTS9-AS1) decreased with increasing risk score, while the expression of risk lncRNAs (CASC8, LUCAT1, AC099850.4, FALEC, AC096531.2, FAM66C, FOXD2-AS1, LINC01559, and AC010186.3) increased expression (**Figures 4J-4K**). These findings suggested that this m6A-related prognostic lncRNAs signature has robust and stable predictive power.

m6A-related lncRNA prognostic signature was an independent prognostic factor in KIRP

Univariate Cox regression analysis revealed that gender, clinical stage, and risk score were associated with the prognosis of KIRP patients in the training cohort (**Figure 5A**, all $p< 0.01$). Multivariate Cox regression analysis showed that the risk score was still significantly correlated with the prognosis of KIRP

patients in the training cohort (**Figure 5B**, p = 0.003). In the test cohort, both univariate and multivariate regression analyses indicated that stage and risk scores were markedly correlated with prognostic factors in patients with KIRP (**Figures5C-5D**). Subsequently, based on these independent prognostic factors, a nomogram was developed to quantify the prediction of individual survival probability at 1, 2, and 3 years. The C-index for the nomogram associated with clinical parameters was 0. 868 in the training cohort (**Figure 5E**). The calibration curves showed that the predicted overall survival was consistent with the actual observations at three years in the training cohort (**Figure 5G**) and the test cohort (**Figure 5H**). Also, a nomogram of 1-, 3-, and 5-year overall survival rates based on m6A-related prognostic lncRNAs were determined using the rms package, and the C-index for the nomogram was 0. 888 in the training cohort (**Figure 5F**). Calibration curves showed agreement between predicted outcomes and actual survival, and similar results were obtained in the test cohort (**Figures 5I-5J**). The predictive power of the nomogram was similar to that of the ROC curve, indicating that the m6A-related prognostic lncRNAs model has high reliability. Furthermore, we performed the stratified survival analysis to assess the predictive power of m6A-related prognostic lncRNAs in KIRP patients with different clinicopathological parameters. In each subgroup, high-risk patients (especially men or women aged <= 60 years old) had lower overall survival than low-risk patients (**Figures 6A-6C**). Among KIRP patients with tumor grade 1-2 (**Figure 6D**, p= 0.045), tumor grade 3-4 (**Figure 6E**, p= 0.011), pT1-2 (**Figure 6F**, p= 0.012), pT3-4 (**Figure 6G**, p= 0.030), pN0 **(Figure 6H**, p= 0.007), pN1 **(Figure 6I**, p= 0.041), pM0 (**Figure 6J**, p< 0.001), stage I-II (**Figure 6K,** p= 0.045) and stage III-IV (**Figure 6L,** p= 0.011), the high-risk group had a worse prognosis than the low-risk group. These clinical data analyses demonstrated that m6A-related lncRNA prognostic signaturehad a good predictive performance.

m6A-related prognostic lncRNAs signatures correlated with clinicopathology and TME immune activity

To further disclose the correlation between clinical featuresand the prognostic risk models, the heatmap showed the high-risk and low-risk groups differed in pN stage, pM stage, pT stage, clinical stage, grade, gender, and cluster subtype (**Figure 7A**). The risk score also improved markedly as the clinical stage increased from stage I-II to stage III-IV (**Figure 7B**, p= 5.4e-09). Likewise, KIRP patients with pT3-T4, pN1-N2, and M1 had higher risk scores than T1-T2, N0, and M0 (**Figures 7C-8E**, all p< 0.01). The men, high-grade, and cluster 2 had higher risk scores than females and low-grade (**Figures 7F-7G**, all p< 0.01), and high-risk patients tended to be classified into cluster 2 (**Figure 7H**). These findings suggested that risk scores involving m6A-related prognostic lncRNA signatures were significantly associated with clinical characteristics in patients with KIRP.

We then comprehensively investigated the correlation between the risk score of m6A-related prognostic lncRNAs and immune cell infiltration. By combining differential and correlation analyses, we identified three types of immune cells correlated with risk scores involving m6A-related prognostic lncRNA signatures. The abundance of M2 macrophages was negatively correlated with the risk score (**Figure 8A**, p= 0.00059), and the abundance of M1 macrophages (**Figure 8B**, p= 0.00021) and plasma cells (**Figure 8C**, p= 0.049) was positively associated with the risk score. The expression level of immune checkpoint genes in high-risk and low-risk groups was also explored, the expression levels of HAVCR2 (p=

0.039) decreased, and LAG3 (p= 0.04) were increased in the high-risk group compared with the low-risk group (**Figures 8D, 8E).** These data indicated that the m6A-related lncRNAs prognostic features were associated with the KIRP immune microenvironment. Finally, we compared drug susceptibility to TKIs, chemotherapy, and targeted drugs, including sunitinib, axitinib, sorafenib, rapamycin, pazopanib, temsirolimus, and gemcitabine between risk groups. Risk stratification was significantly associated with sensitivity to sunitinib, rapamycin, pazopanib, and gemcitabine (**Figures 8F-8L**). These data showed that the risk scores of m6A-related lncRNAs prognostic signature was the potential targets of multiple drugs and had important significance for guiding the treatment of KIRP patients.

Discussion

m6A methylation, a common form of mRNA modification and metabolism, plays a crucial role in regulating gene expression at the post-transcriptional level [12]. Numerous recent studies have emphasized that aberrant m6A methylation regulates various biological processes, including cell differentiation, immune responses, mammalian development, tumor formation and metastasis, stem cell renewal, and has profound effects on the progression of malignant tumors [13–15]. Many studies have reported the pathological significance of m6A in cancers, and m6A-related genes could be used as prognostic markers to predict survival [16–17]. Given the limited predictive power of traditional prognostic models, prognostic models of m6A-related lncRNAs might improve the understanding and management of tumors, including KIRP. The analysis of m6A-related lncRNAs in the KIRP cohort had vital implications for guiding the direction and goals of KIRP research. In our study, we performed a comprehensive KIRP RNA-seq analysis using the TCGA database to establish an m6A-related lncRNA prognostic signature to predict the prognosis of KIRP patients. We further analyzed the correlation of m6A-related lncRNA signatures in KIRP patients with the TME and tumor drug treatment sensitivity. In this study, by systematically screening and identifying target lncRNAs, we created a reliable prognostic model with satisfactory predictive power for KIRP outcomes.

This study first recruited 289 KIRP patients from the TCGA dataset and identified 1387 m6A-related lncRNAs discerned as m6A-related lncRNAs by constructing a co-expression network. Then, m6A-related prognostic lncRNA data were extracted, and univariate Cox regression analysis indicated that 32 m6A-related lncRNAs served as prognostic features of overall survival in KIRP patients. The expression of 32 m6A-related prognostic lncRNAs differed between renal papillary cell carcinoma tissues and normal tissues. The m6A modification of lncRNAs plays a crucial role in altering the structure of lncRNAs and affects their interactions with proteins by mediating the repression of gene transcription and altering their subcellular distribution [18]. These data explained our findings well, as some m6A-related lncRNAs were overexpressed in tumors to act as oncogenes, while some were highly expressed in normal tissues to act as tumor suppressors.

Subsequently, the TCGA-KIRP cohort was divided into two clusters by the consistent expression of m6A-related prognostic lncRNAs. Interestingly, KIRP patients in cluster 2 had lower overall survival than cluster 1, suggesting that the landscape of prognostic m6A-related lncRNAs affects the prognosis of KIRP

patients. KIRP patients in cluster 2 had higher immune, stroma, and ESTIMATE scores than cluster 1, indicating that the TME in cluster 2 is better than that in cluster 1. These results were consistent with previous studies, which revealed that tumor patients with high immuneScore and stromalScore had poorer overall survival rates [19–20]. Afterwards, we identified the expression of immune checkpoint genes in two subtypes and the correlation of these molecules with m6A-related lncRNAs; the results showed that the expression level of PD-L1, HAVCR2, LAG3, PDCD1LG2, SIGLEC15, and TIGIT in cluster 2 were higher than that in cluster 1, indicating that the expression pattern of m6A-related lncRNAs was significantly associated with immunity and tumorigenesis. Previous studies have shown that multiple lncRNAs indirectly regulate the expression of immune checkpoint genes, thereby affecting the survival of cancer patients [21]. We considered that the expression profile of m6A-related prognostic lncRNAs in cluster 2 might enhance the expression of immune checkpoint genes, resulting in decreased overall survival. It has also been reported that patients with high PD-L1 expression treated with PD-1 inhibitors were more effective than platinum-based doublet chemotherapy, indirectly suggesting that PD-1 inhibitors may be an effective therapy for patients in cluster 2 [22].

To further improve overall survival and progression risk prediction in KIRP patients, we incorporated 14 m6A-related prognostic lncRNAs into m6A-related lncRNAs prognostic signature by LASSO Cox regression. Fourteen m6A-related prognostic lncRNAs were stratified into low- and high-risk groups and exhibited remarkable predictive performance. The m6A-associated lncRNA prognostic molecules included CASC8, LUCAT1, AC099850.4, FALEC, AC096531.2, FAM66C, FOXD2-AS1, LINC01559, AC010186.3, AL133355.1, ZKSCAN7 – AS1, AC135050.6, ADAMTS9 – AS1 and DSG2 – AS1. Like FOXD2-AS1, METTL3-mediated FOXD2-AS1 has been reported to accelerate cervical cancer progression by recruiting lysine-specific demethylase 1 (LSD1) to the promoter region p21 to silence its transcriptional abundance [23]. Multivariate Cox regression analysis showed that m6A-related prognostic lncRNAs signature was an independent prognostic factor with potential value in predicting the prognosis and risk of tumor progression for KIRP patients. The predictive power of this feature was validated in patients stratified according to clinicopathological parameters. By integrating age, tumor grade, and stage and m6A-related lncRNAs expression, we constructed two quantitative nomograms that were highly accurate and reliable in estimating the survival of KIRP patients. Importantly, cluster 2 with worse overall survival had a higher risk score than cluster 1 with longer overall survival, thus indicating the consistency of the two methods for predicting prognosis in KIRP patients. Previous studies have also shown some novel prognostic features of malignancies. Chen et al. determined a signature based on m6A RNA methylation regulators for predicting overall survival in malignancies and showed good prediction efficiency, consistent with our model [24].

Many studies have shown that m6A modifications and lncRNAs can regulate cancer immunity, including immune cell infiltration in the TME and immune resistance and activation, affecting the prognosis of tumor patients [25–27]. Also, TKIs combined with immune checkpoint inhibitors have been recommended as a common treatment for metastatic KIRC, and TME is actively involved in the efficacy of these treatments [28]. Our findings suggest that m6A-related lncRNAs play a crucial role in the immune status of KIRP patients, so we further analyzed the association between m6A-related lncRNAs and TME immune

activity. Infiltration of immune cells (memory B cells, resting CD4 memory T cells, and resting mast cells) was highly clustered in cluster 1. Other immune cells (naive memory B cells, T cell CD8, activated CD4 memory T cells, follicular helper T cells, and macrophages M1) were significantly increased in KIRP patients in cluster 2 compared with cluster 1. Likewise, the risk score was positively correlated with infiltration levels of M1 macrophages and HAVCR2 expression and negatively associated with M2 macrophages, plasma cells, and LAG3 expression. These data indicated that higher proportions of M1 macrophages and LAG3 expression and lower proportions of M2 macrophages, plasma cells, and HAVCR2 expression might increase the risk of poor prognosis in KIRP patients. Notably, our data were similar to previous results, indicating that tumor-infiltrating immune cells in the high-risk group were associated with a high risk of disease recurrence and poorer overall survival outcomes [29–30]. We speculated that higher immunosuppression and lower immunoreactivity in the TME were common factors contributing to poorer prognosis in high-risk KIRP patients. The signatures of TME cell infiltration in KIRP patients were correlated with specific m6A-related lncRNAs signatures and might contribute to the development of personalized novel immunotherapies. Also, the clinical utility of the combination of TKIs, chemotherapy, and targeted drugs in the metastatic renal tumor is being extensively studied [31]. Risk subgroups in our study were prominently associated with drugs sensitivity to sunitinib, axitinib, sorafenib, rapamycin, pazopanib, temsirolimus, and gemcitabine, suggesting that this m6A-related prognostic lncRNAs signature has potential roles in estimating response to multiple drugs.

Nonetheless, the current study has some limitations. First, external validation based on the KIRP samples and independent clinical data was required to validate our findings for clinical KIRP patients. Furthermore, we established an m6A-related lncRNA prognostic signature to predict the prognosis of KIRP patients and the correlation of the m6A-related lncRNA signature with the TME in KIRP. However, the specific functions and mechanisms of m6A-related prognostic lncRNA signatures in KIRP remained undetermined, and experimental studies were needed to validate our findings. The regulatory mechanism of m6A-related prognostic lncRNAs deserved further study to improve the precise prediction of prognosis and immunotherapy in KIRP patients.

Conclusion

This study demonstrated that m6A-related prognostic lncRNAs signature played a critical role in predicting the prognosis of patients with KIRP and their role in the heterogeneity and complexity of the TME. Our findings may help to study the function and mechanism of KIRP tumorigenesis and to determine treatment strategies and efficacy in patients with KIRP.

Materials And Methods

Data collection and processing

RNA-sequencing transcriptome data and clinical data of KIRP patients were downloaded from The Cancer Genome Atlas (TCGA) database, and raw count data for 289 KIRP samples and 32 normal tissues

were collected using Perl version 5.24.1 software. The expression data of lncRNAs and genes in the transcriptome were extracted according to the genotype biotypes. Then, relevant clinical information on KIRP patients was obtained, including age, grade, and survival status. KIRP patients with missing status or no overall survival value were excluded to reduce statistical bias in this analysis. According to the National Cancer Institute guidelines from Dec. 2015, the study had no ethical implications and did not require ethics committee approval.

Selection of m6A-related lncRNAs associated with prognosis of KIRP patients

Expression matrices of 23 m6A-related genes (METTL3, METTL14, METTL16, WTAPI, VIRMA, ZC3H13, RBM15, RBM15B, YTHDC1, YTHDC2, YTHDF1, YTHDF2, YTHDF3, HNRNPC, FMR1, LRPPRC, HNRNPA2B1, IGFBP1, IGFBP2, IGFBP3, RBMX, FTO, and ALKBH5) were obtained based on the publication [11]. M6A-related lncRNAs were extracted with the criteria of |Pearson R|> 0.3 and p< 0.001 by co-expression analysis of m6A-related genes expression and lncRNAs using the Pearson correlation coefficient. These data were visualized in the network graph and Sankey diagram using the Cytoscape software and R ggalluvial package. LncRNAs were then combined with clinical survival data, and a univariate Cox regression analysis was performed using the survival package to identify m6A-associated prognostic lncRNAs ($p < 0.001$). Furthermore, differences in m6A-related prognostic lncRNAs expression between tumor and normal samples were ascertained using the limma, pheatmap, and ggpubr packages and displayed with heatmaps and boxplots.

Consensus clustering analysis of m6A-related lncRNAs

To screen the potential features of m6A-related lncRNAs associated with the prognosis, KIRP patients were clustered into various subtypes via the ConsensusClusterPlus and limma packages with pfeature =1, resample rate =0.8, and iterations =50. The optimal k value (k= 2) was determined to obtain relatively stable clusters, namely clusters 1 and 2. Survival analysis and chi-square or Fisher's exact test were applied to compare prognosis between clusters and determine the relationship between clinical characteristics and clusters. Heatmap was created using the R pheatmap package to visualize the differential expression of lncRNAs and clinical features in clusters 1 and 2.

Correlation of m6A-related lncRNAs with the TME and immune cell infiltration

We used the CIBERSORT algorithm to evaluate the immune cell infiltration in different clusters. Immune, stromal, and ESTIMATE scores were calculated using the ESTIMATE algorithm by the limma and estimate packages for each KIRP patient. Immune cell infiltration could be estimated using RNA-seq data, and $p < 0.05$ indicated that the inferred cellular composition was reliable. Differences in the infiltration of 22 immune cells from different clusters were analyzed and visualized using the vioplot package. To further explore the correlation between m6A-related lncRNAs with tumor immune checkpoint inhibitors, we studied a variety of tumor immune checkpoint inhibitory molecules, including PD-L1, CTLA-4, LAG-3, HAVCR2 (TIM-3), PDCD1LG2, SIGLEC15, and TIGHT. Wilcoxon's test was utilized to examine differences in the expression of immune molecules, immune, stromal, and ESTIMATE scores between the two

clusters, and we plotted the results as boxplots ($p< 0.05$). The correlations of m6A-related prognostic lncRNAs and tumor immune checkpoint inhibitory molecules in KIRP patients were detected and plotted by corrplot package.

Construction and validation of a risk model for m6A-related prognostic lncRNAs

KIRP patients with survival data from the TCGA database were randomly divided into the training and test groups using the R caret, glmnet, surviner, and survival packages. LASSO regression analysis was used to construct a prognostic model. The risk score formula for each patient was as follows: risk score = $\text{score} = \sum_{i=1}^{n} Coefi * Expi$, where Coefi represents the coefficient, and Expi represents the expression value of m6A-related lncRNA. Then, the training and test groups were divided into the high-risk and low-risk groups according to the median score. Kaplan-Meier survival analysis and the log-rank test were used to analyze the prognostic significance of the high- and low-risk groups using the survival package ($p< 0.05$). A time-dependent receiver operating characteristic (ROC) curve was applied to estimate the model's predictive accuracy for predicting the prognostic signatures of m6A-related lncRNAs using the "survivalROC" packages. We depicted risk curves for risk scores of KIRP patients in the training and testing cohorts and assessed survival status and risk associated with m6A-related prognostic lncRNAs. Next, nomograms based on clinical factors and gene expression were constructed and analyzed using multiple regression with a comprehensive evaluation using the concordance index (C-index) and calibration curve. Univariate and multivariate Cox regression analyses were performed to investigate whether risk scores could be independent prognostic factors and clinical features for the prognosis of patients with KIRP. Subsequently, survival analyses were performed to elucidate the predictive power of risk scores in subgroups stratified by age, sex, grade, stage, and TNM stage. We analyzed the correlations between risk scores and clinicopathological features to assess the ability of the model to predict KIRP progression.

Correlation between m6A-related prognostic lncRNA signatures and TME immune activity

We downloaded data for different cancer cell lines from the NCI-60 database (https://discover.nci.nih.gov/cellminer/home.do). A comprehensive analysis of m6A-related prognostic lncRNA signatures was performed to determine their relationship with common drug sensitivities in KIRP treatment. We then investigated differences in immune checkpoint expression between high- and low-risk patients. The correlation between risk scores and tumor-infiltrating immune cells was evaluated using the Wilcoxon rank-sum test and Spearman correlation analysis and presented as boxplots.

Statistical analysis

All statistics were analyzed and performed using R version 4.1.3 and Perl version 5.24.1. M6A-related lncRNAs and tumor-related immune cells were compared using the Wilcoxon rank-sum test. Pearson correlation analysis was performed to identify m6A-related prognostic lncRNAs signatures. Survival curves were drawn using the Kaplan-Meier method and log-rank test to compare the differences in overall

survival between groups. Differences in parameters between two subgroups were evaluated by independent t-test. The associations between clinicopathological parameters, immune scores, clustering, and m6A-related prognostic lncRNAs signatures were analyzed by the Chi-square test or Fisher's exact test. Univariate and multivariate Cox regression analyses were applied to analyze the independent predictive role of the risk scores integrated with other clinical features of patients with KIRP. A P-value < 0.05 was indicated statistical significance.

Declarations

Acknowledgements

The authors sincerely acknowledge the publicly available TCGA (https://portal.gdc.cancer.gov/) database.

Authors' contributions

XD, MZ, and ZH are the principal investigator. XD and JZconducted statistical analysis and data management. XD, ZW, and ZWedited and revised the manuscript. All authors read and approved the final manuscript.

Funding

The study was supported by grants from China's National Natural Science Foundation (82103257).

Availability of data and materials

The raw data of this study are derived from the TCGA database (https://portal.gdc.cancer.gov/) which are publicly available databases.

Ethics approval and consent to participate

Not necessary.

Consent for publication

Not applicable.

Competing interests

The authors declare that they have no competing interests.

References

1. Sung Hyuna, Ferlay Jacques, Siegel Rebecca L, et al. Global Cancer Statistics 2020: GLOBOCAN Estimates of Incidence and Mortality Worldwide for 36 Cancers in 185 Countries. CA Cancer J Clin,

2021; 71: 209–249. doi: 10.3322/caac.21660.

2. Marchetti Andrea, Rosellini Matteo, Mollica Veronica, et al. The Molecular Characteristics of Non-Clear Cell Renal Cell Carcinoma: What's the Story Morning Glory? Int J Mol Sci. 2021; 22(12):6237. doi: 10.3390/ijms22126237.
3. Yu J, Mao W, Sun S, et al. Identification of an m6A-Related lncRNA Signature for Predicting the Prognosis in Patients With Kidney Renal Clear Cell Carcinoma. Front Oncol. 2021; 11:663263. doi: 10.3389/fonc.2021.663263.
4. Gu Y, Niu S, Wang Y, et al. DMDRMR-Mediated Regulation of m6A-Modified CDK4 by m6A Reader IGF2BP3 Drives ccRCC Progression. Cancer Res. 2021; 81(4):923–934. doi: 10.1158/0008-5472.CAN-20-1619.
5. Strick Alexander, von Hagen Felix, Gundert Larissa, et al. The N-methyladenosine (m6A) erasers alkylation repair homologue 5 (ALKBH5) and fat mass and obesity-associated protein (FTO) are prognostic biomarkers in patients with clear cell renal carcinoma. BJU Int, 2020; 125: 617–624. doi: 10.1111/bju.15019.
6. Xue Lei, Li Jun, Lin Yihui, et al. m6A transferase METTL3-induced lncRNA ABHD11-AS1 promotes the Warburg effect of non-small-cell lung cancer. J Cell Physiol. 2021; 236: 2649–2658. doi: 10.1002/jcp.30023.
7. Shen Danyang, Ding Lifeng, Lu Zeyi, et al. METTL14-mediated Lnc-LSG1 m6A modification inhibits clear cell renal cell carcinoma metastasis via regulating ESRP2 ubiquitination. Mol Ther Nucleic Acids. 2022; 27: 547–561. doi: 10.1016/j.omtn.2021.12.024.
8. Sun Zhuolun, Jing Changying, Xiao Chutian, et al. Prognostic risk signature based on the expression of three m6A RNA methylation regulatory genes in kidney renal papillary cell carcinoma. Aging (Albany NY). 2020; 12: 22078–22094. doi: 10.18632/aging.104053.
9. Wang Y, Li N, Tian D, et al. Analysis of m6A-Related lncRNAs for Prognosis Value and Response to Immune Checkpoint Inhibitors Therapy in Hepatocellular Carcinoma. Cancer Manag Res. 2021; 13:6451–6471. doi: 10.2147/CMAR.S322179.
10. Weng C, Wang L, Liu G, et al. Identification of a N6-Methyladenosine (m6A)-Related lncRNA Signature for Predicting the Prognosis and Immune Landscape of Lung Squamous Cell Carcinoma. Front Oncol. 2021; 11:763027. doi: 10.3389/fonc.2021.763027.
11. Y. Jin, Z. Wang, D. He, et al. Analysis of m6A-related signatures in the tumor immune microenvironment and identification of clinical prognostic regulators in adrenocortical carcinoma. Frontiers in Immunology. 2021; 12:637933. doi: 10.3389/fimmu.2021.637933.
12. Liu Li, Li Hui, Hu Dingyu, et al. Insights into N6-methyladenosine and programmed cell death in cancer. Mol Cancer. 2022; 21: 32. doi: 10.1186/s12943-022-01508-w.
13. Song Hao, Song Jiaxi, Cheng Ming, et al. METTL3-mediated mA RNA methylation promotes the anti-tumour immunity of natural killer cells. Nat Commun. 2021; 12: 5522. doi: 10.1186/s13046-021-02096-1.

14. Cui Yuanbo, Zhang Chunyan, Ma Shanshan, et al. RNA m6A demethylase FTO-mediated epigenetic up-regulation of LINC00022 promotes tumorigenesis in esophageal squamous cell carcinoma. J Exp Clin Cancer Res. 2021; 40: 294. doi: 10.1186/s13046-021-02096-1.
15. An Yuanyuan, Duan Hua. The role of m6A RNA methylation in cancer metabolism. Mol Cancer. 2022; 21: 14. doi: 10.1186/s12943-022-01500-4.
16. Xu Qiong-Cong, Tien Yi-Chih, Shi Yin-Hao, et al. METTL3 promotes intrahepatic cholangiocarcinoma progression by regulating IFIT2 expression in an m6A-YTHDF2-dependent manner. Oncogene. 2022 Jan 29. doi: 10.1038/s41388-022-02185-1.
17. Li Wei, Gao Yingchao, Jin Xiaojing, et al. Comprehensive analysis of N6-methylandenosine regulators and m6A-related RNAs as prognosis factors in colorectal cancer. Mol Ther Nucleic Acids. 2022; 27: 598–610. doi: 10.1016/j.omtn.2021.12.007.
18. Lan Yufei, Liu Boyang, Guo Hongbo. The role of MA modification in the regulation of tumor-related lncRNAs. Mol Ther Nucleic Acids. 2021; 24: 768–779. doi: 10.1016/j.omtn.2021.04.002.
19. Wu Zhongguang, Zhang Xiaobo, Chen Dongjie, et al. N6-Methyladenosine-Related LncRNAs Are Potential Remodeling Indicators in the Tumor Microenvironment and Prognostic Markers in Osteosarcoma. Front Immunol, 2021; 12: 806189. doi: 10.3389/fimmu.2021.806189.
20. Huang Shenglan, Zhang Jian, Lai Xiaolan, et al. Identification of Novel Tumor Microenvironment-Related Long Noncoding RNAs to Determine the Prognosis and Response to Immunotherapy of Hepatocellular Carcinoma Patients. Front Mol Biosci. 2021; 8: 781307. doi: 10.3389/fmolb.2021.781307.
21. Jin Chen, Li Rui, Deng Tuo, et al. Identification and Validation of a Prognostic Prediction Model of m6A Regulator-Related LncRNAs in Hepatocellular Carcinoma. Front Mol Biosci. 2021; 8: 784553. doi: 10.3389/fmolb.2021.784553.
22. Aguilar, E. J, Ricciuti, B, Gainor, J. F, et al. Outcomes to First-Line Pembrolizumab in Patients with Non-small-cell Lung Cancer and Very High PD-L1 Expression. Ann. Oncol. 2019; 30 (10): 1653–1659. doi:10.1093/annonc/mdz288
23. Ji Fei, Lu Yang, Chen Shaoyun, et al. m6A methyltransferase METTL3-mediated lncRNA FOXD2-AS1 promotes the tumorigenesis of cervical cancer. Mol Ther Oncolytics. 2021; 22:574–581. doi: 10.1016/j.omto.2021.07.004.
24. Chen, J, Yu, K, Zhong, G, and Shen, W. Identification of a m6A RNA Methylation Regulators-Based Signature for Predicting the Prognosis of clear Cell Renal Carcinoma. Cancer Cel Int. 2020; 20, 157. doi:10.1186/s12935-020-01238-3
25. Deng W, Wang G, Deng H, et al. The Role of Critical N6-Methyladenosine-Related Long Non-Coding RNAs and Their Correlations with Immune Checkpoints in Renal Clear Cell Carcinoma. Int J Gen Med. 2021; 14:9773–9787. doi: 10.2147/IJGM.S344771.
26. Jiang Z, Zhang Y, Chen K, et al. Integrated Analysis of the Immune Infiltrates and PD-L1 Expression of N6-Methyladenosine-Related Long Non-Coding RNAs in Colorectal Cancer. Int J Gen Med. 2021; 14:5017–5028. doi: 10.2147/IJGM.S327765.

27. Gu, Y, Wu, X, Zhang, J, et al. The Evolving Landscape of N6-Methyladenosine Modification in the Tumor Microenvironment. Mol. Ther. 2021; 29, 1703–1715. doi:10.1016/j.ymthe.2021.04.009.
28. Simonaggio, A, Epaillard, N, Pobel, C, et al. Tumor Microenvironment Features as Predictive Biomarkers of Response to Immune Checkpoint Inhibitors (ICI) in Metastatic clear Cell Renal Cell Carcinoma (mccRCC). Cancers. 2021; 13, 231. doi:10.3390/ cancers13020231
29. Li Z, Li Y, Zhong W, et al. m6A-Related lncRNA to Develop Prognostic Signature and Predict the Immune Landscape in Bladder Cancer. J Oncol. 2021; 2021:7488188. doi: 10.1155/2021/7488188.
30. Langhans B, Nischalke HD, Krämer B, et al. Role of regulatory T cells and checkpoint inhibition in hepatocellular carcinoma. Cancer Immunol Immunother. 2019; 68(12):2055–2066. doi: 10.1007/s00262-019-02427-4.

Tables

Table 1. Identification of 32 m6A-related prognostic lncRNAs in KIRP using univariate Cox regression analysis

Gene	HR	HR.95L	HR.95H	p-value
AC087289.1	7.859638061	2.469898118	25.01071198	0.000481399
CASC8	4.237434475	2.192102936	8.191153178	1.76E-05
AC005740.3	3.791348521	1.799075291	7.989839938	0.000458248
LUCAT1	1.829878919	1.488291096	2.24986689	9.94E-09
AC114763.1	40.80191901	6.896584733	241.3943508	4.33E-05
SCAT8	1.7132271	1.306747804	2.246146567	9.78E-05
AP005899.1	1.880035233	1.368388355	2.582989299	9.82E-05
AC099850.4	1.470141101	1.317665511	1.640260627	5.28E-12
AC099850.2	18.24603218	6.137891888	54.23974494	1.75E-07
ENTPD3-AS1	0.463968437	0.301197634	0.714702529	0.000494533
CCDC13-AS1	0.449255812	0.28722022	0.702703956	0.000455258
AP002840.2	0.655597832	0.515640712	0.833542633	0.000568961
TMPO-AS1	2.886951682	1.692753535	4.923628776	9.92E-05
FALEC	11.50882485	3.554760814	37.26074869	4.58E-05
AC021851.1	5.417889845	2.001075847	14.66887446	0.00088421
AC096531.2	2.264494122	1.403974511	3.652440688	0.00080488
FAM66C	3.904110311	1.925767262	7.914807579	0.000158456
AL078644.2	2.018940337	1.362052656	2.992630327	0.000467535
CT66	2.977551272	1.754567175	5.052990677	5.27E-05
AF117829.1	5.56646459	2.799498601	11.06824201	9.80E-07
AC090181.2	2.413239015	1.470286127	3.960945042	0.000492854
AF127577.4	4.124549154	2.210753563	7.695071043	8.46E-06
LINC00630	8.981884147	2.729430631	29.55716915	0.00030363
AP001267.3	0.069015608	0.018049689	0.263891196	9.35E-05
AC096642.1	2.415570597	1.462648009	3.989327081	0.000570007
FOXD2-AS1	1.305509811	1.190062722	1.432156336	1.67E-08
FBXL19-AS1	1.39477625	1.162159277	1.67395367	0.000351164
SNHG4	1.39144149	1.185648842	1.632953495	5.23E-05

AC091057.1	18.77460245	5.381396498	65.50078537	4.23E-06
AC004870.2	1.281266221	1.140220795	1.43975898	3.11E-05
AC010186.3	3.341941452	1.954258453	5.714992638	1.05E-05
RDH10-AS1	3.36950483	1.987949395	5.711193067	6.42E-06

Figures

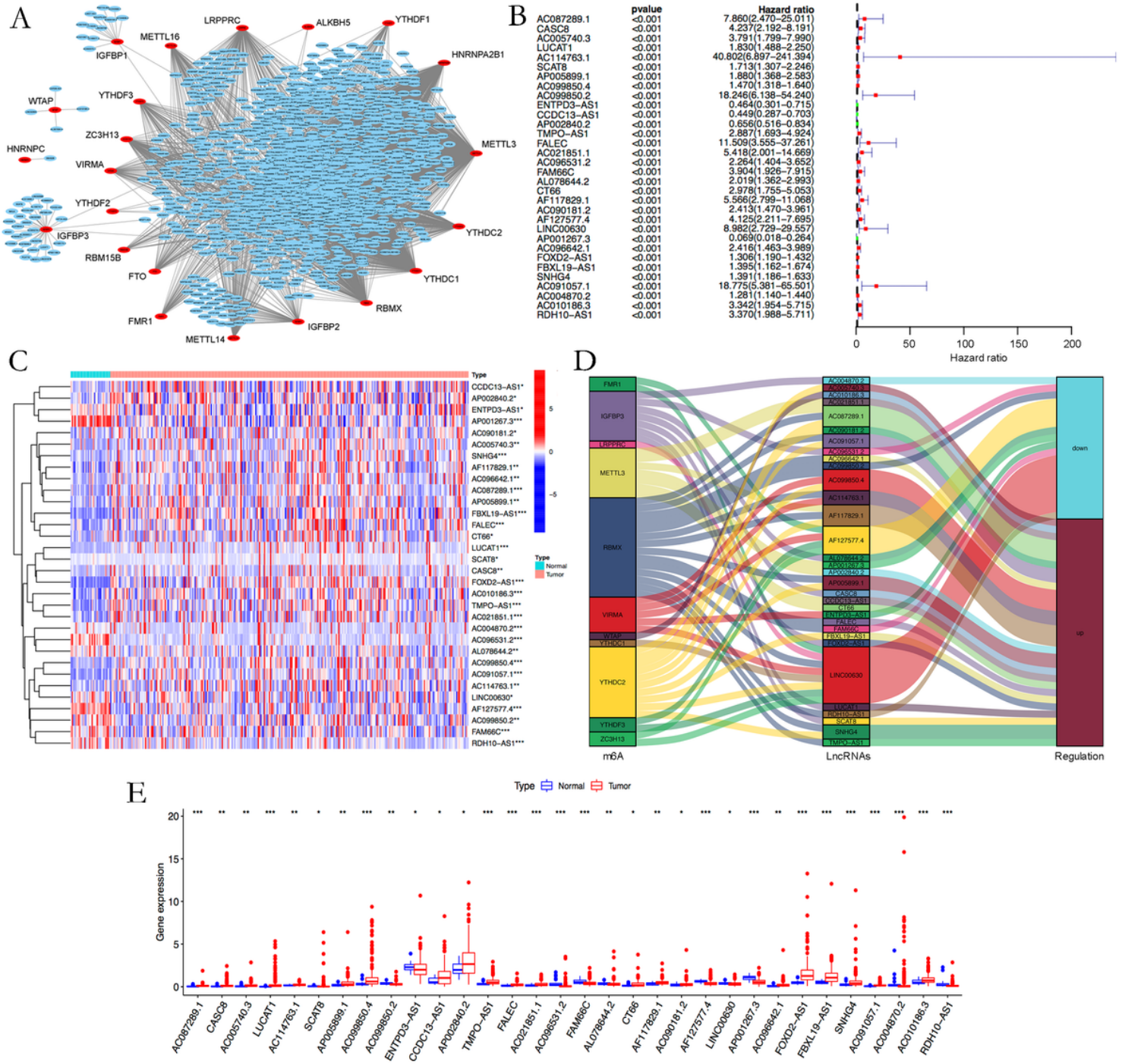

Figure 1

Identification of m6A-related prognostic lncRNAs and their expression in KIRP samples.

(A) Co-expression network of m6A-related genes and lncRNAs in KIRP samples. Red dots represent m6A methylation regulators, and blue dots represent lncRNAs.

(B) Forest plot of 32 m6A-related prognostic lncRNAs identified by univariate Cox regression.

(C) Heatmap of differences in the expression of 32 m6A-related prognostic lncRNAs between tumor tissues and normal tissues. *p < 0.05; **p < 0.01; ***p < 0.001.

(D) Sankey diagram of the correlation of 32 m6A methylation regulators and m6A-related prognostic lncRNAs.

(E) Boxplot of the expression levels of 32 m6A-related prognostic lncRNAs in KIRP tissues and normal tissues. *p < 0.05; **p < 0.01; ***p < 0.001.

Figure 2

Consensus clustering analysis of m6A-related prognostic lncRNAs.

(A) Consensus clustering cumulative distribution function for k= 2 to 9.

(B) Relative change in the area under the cumulative distribution function curve for k= 2 to 9.

(C) Consensus clustering matrix for k = 2.

(D) Kaplan–Meier curves survival analysis of overall survival for KIRP patients in clusters 1 and 2.

(E) The heatmap of clinicopathologic features of the two clusters. Red represents high expression, and blue represents low expression. *p < 0.05; **p < 0.01; ***p < 0.001.

Figure 3

Correlation of m6A-related lncRNAs with the TME and immune cell infiltration in KIRP.

(A) Infiltration levels of 22 immune cell types in the clusters 1 and 2 subtypes in KIRP.

(B-D) KIRP patients in cluster 2 had higher ESTIMATEScore (B), immuneScore (C), and stromalScore (D) than those in cluster 2.

(E–J) Boxplot of the expression level of PD-L1 (E), HAVCR2 (F), LAG3 (G), PDCD1LG2 (H), SIGEC15 (I) TIGIT (J) in cluster 1 and cluster 2 in KIRP. *p < 0.05; **p < 0.01; ***p < 0.001.

(K) Boxplot of the expression level of immune checkpoints genes in KIRP tissues and normal tissues. *p < 0.05; **p < 0.01; ***p < 0.001.

(L) Correlation of 32 m6A-related lncRNAs with differentially expressed immune checkpoint molecules. Red represents a positive correlation, blue represents a negative correlation, and * indicates a statistically significant difference.

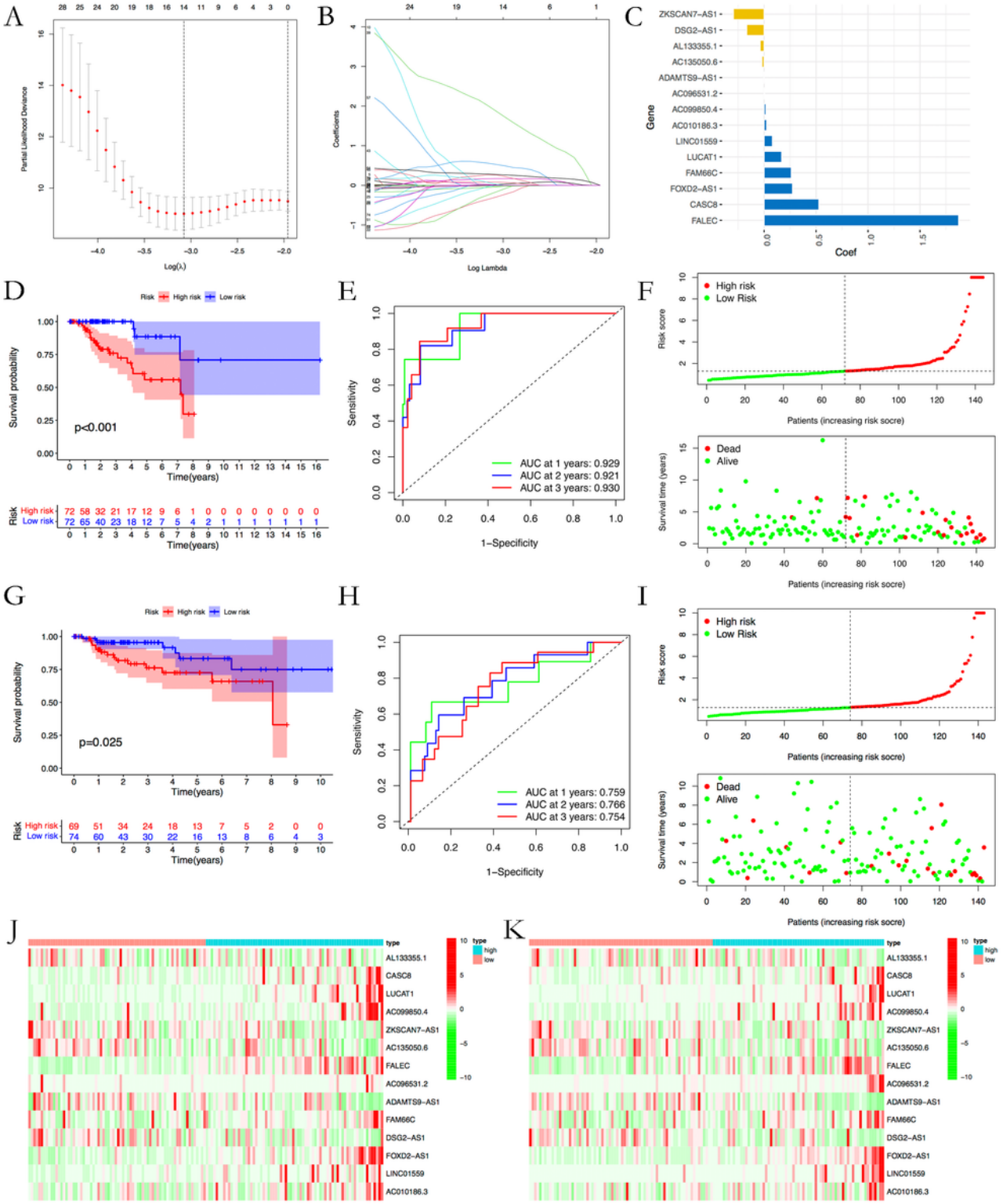

Figure 4

Construction of the risk model of m6A-related prognostic lncRNAs signature in KIRP.

(A-C) LASSO Cox regression analysis determined the 14 m6A-related prognostic lncRNAs and their corresponding coefficients.

(D and G) Survival curve for KIRP patients of the high-risk or low-risk groups in training cohort (D) and test cohort (G).

(E and H) ROC curve for predicting 1-, 2-, and 3-years overall survival rates of high-risk or low-risk in training cohort (E) and test cohort (H).

(F and I) Distributions of risk scores and survival status in the training cohort (F) and the test cohort (I).

(J and K) Heatmap of expression levels of m6A-related prognostic lncRNAs in the training cohort (J) and the test cohort (K).

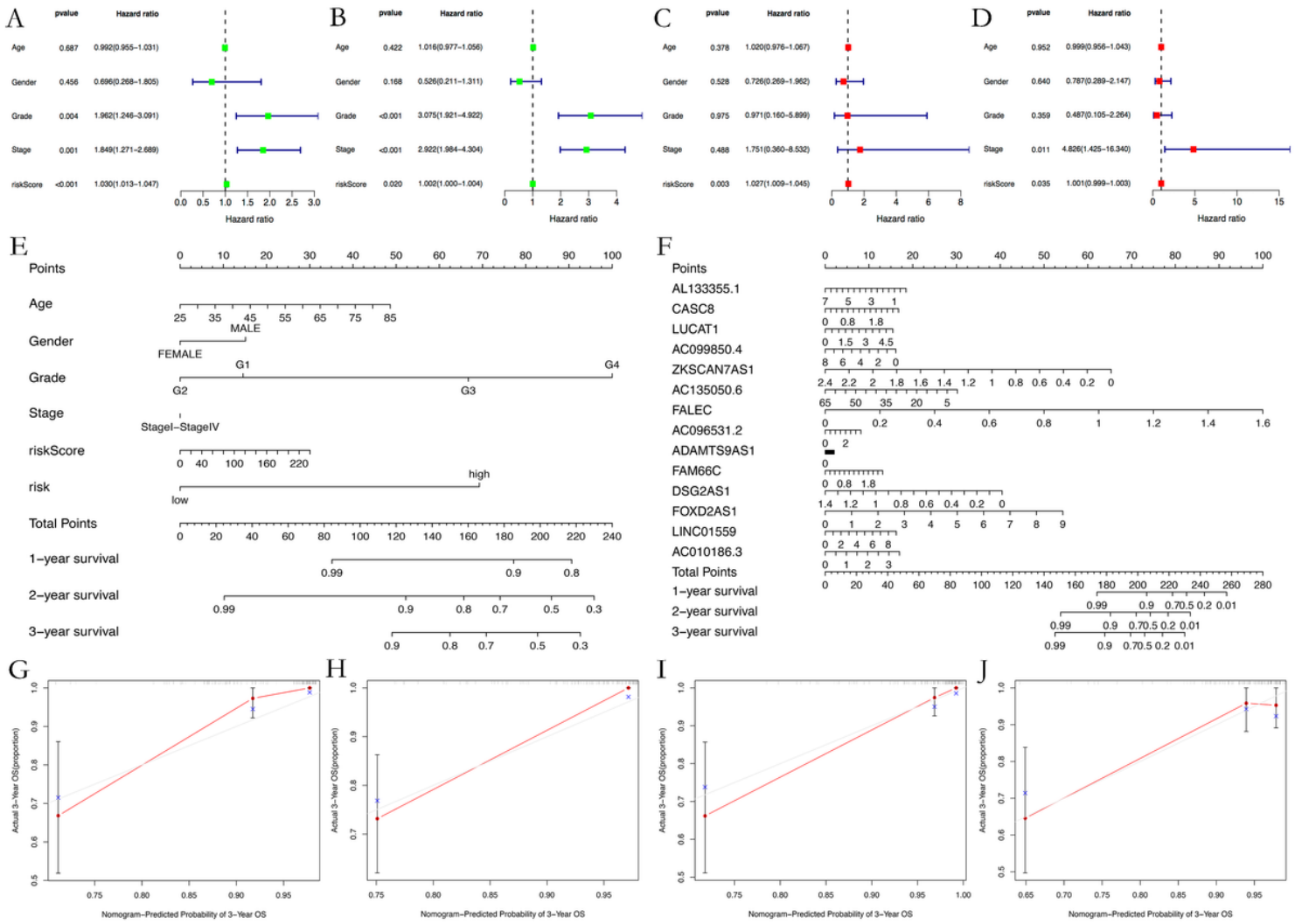

Figure 5

The m6A-related prognostic lncRNAs signature was an independent prognostic factor for the overall survival of KIRP patients.

(A-B) Univariable Cox regression analyses of risk score and clinicopathological features in the training cohort (A) and test cohort (B).

(C-D) Multivariate Cox regression analyses of risk score and clinicopathological features in the training cohort (C) and test cohort (D).

(E) The nomogram for predicting the overall survival of patients with KIRP based on risk score, risk, age, gender, grade, and stage in the training cohort.

(F) The nomogram for predicting the overall survival of patients with KIRP based on m6A-related prognostic lncRNAs in the training cohort.

(G–H) Calibration plots of the nomogram for predicting the probability of overall survival at three years in the training cohort (G) and test cohort (H).

(I-J) Calibration plots of the nomogram for predicting the probability of overall survival at three years in the training cohort (I) and test cohort (J).

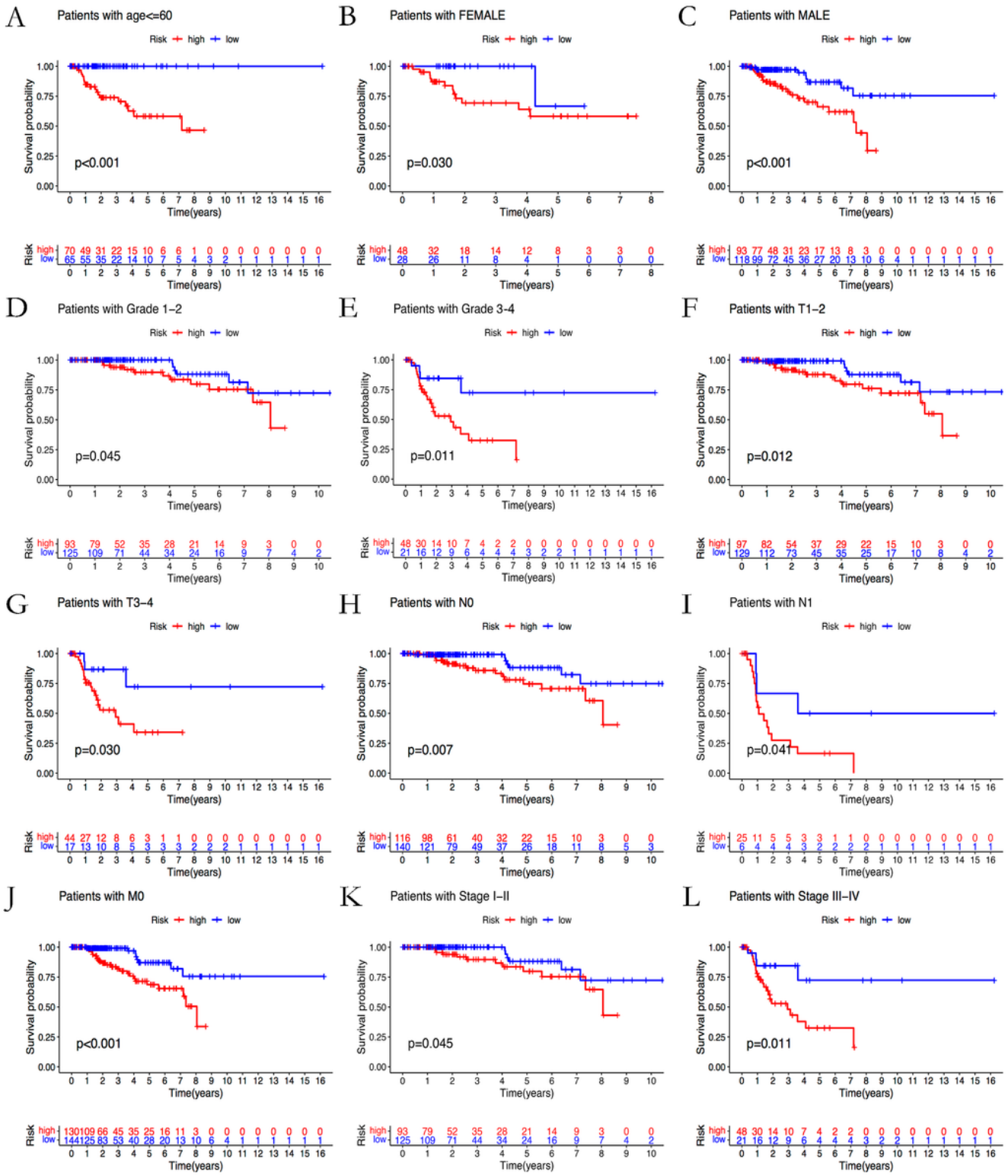

Figure 6

Stratification analysis of risk model survival curve based on the clinicopathological features.

The risk model was applied to evaluate the prognosis of KIRP patients in different clinical groups: age (A), gender (B, C), grade 1-2 (D), grade 3-4 (E), pT1-2 stage (F), pT3-4 stage (G), pN0 stage (H), pN1 stage

(I), pM0 stage (J), stage I-II (K), stage III-IV (L). The survival rate of the low-risk group was higher than that of the high-risk group, all p< 0.05.

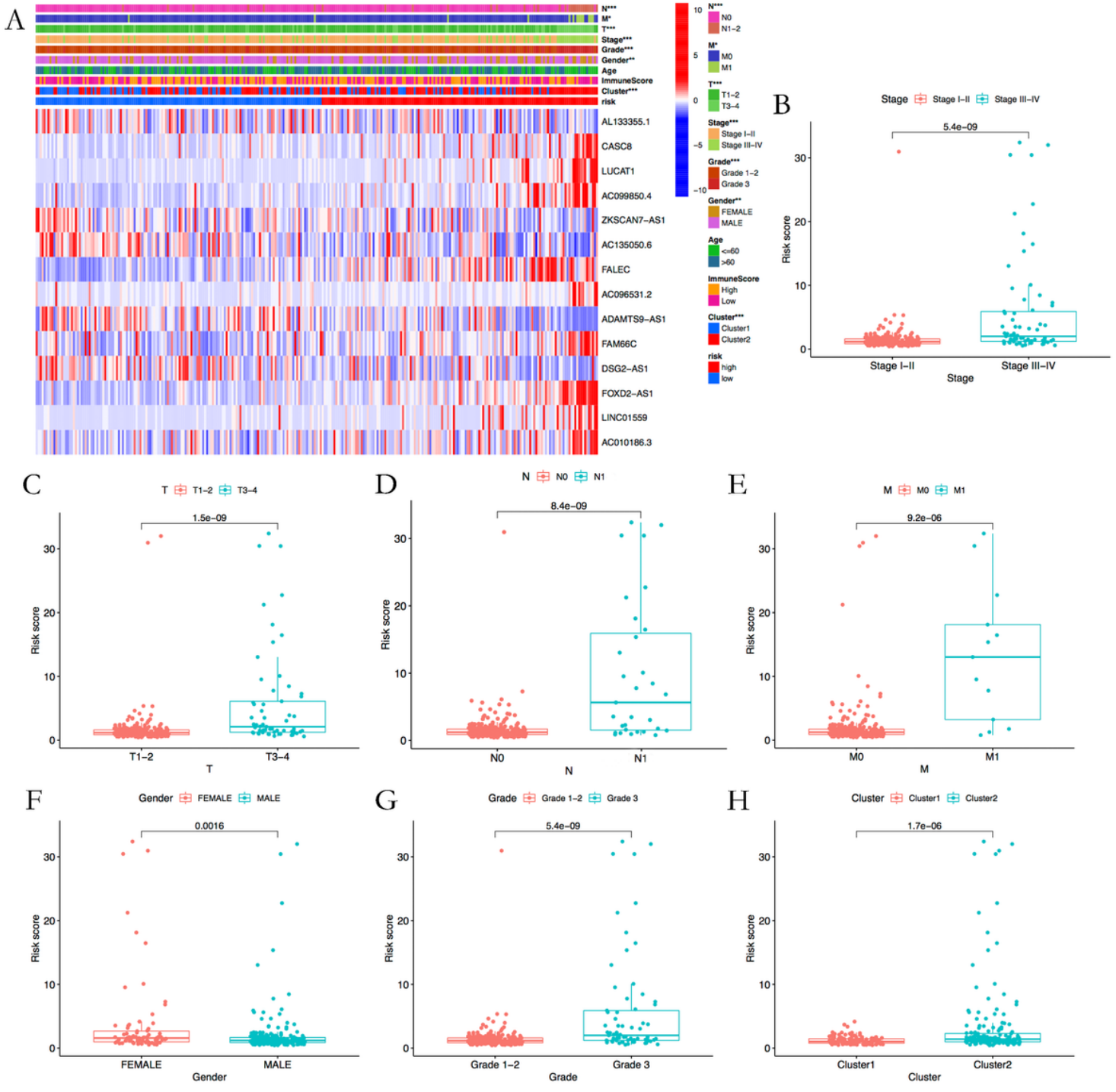

Figure 7

Correlation analysis of risk score and clinicopathological features in KIRP patients.

(A) Heatmap of risk scores and clinical correlation analysis. The risk scores related to pT stage, pN stage, pM stage, stage, grade, gender, and cluster. (*p < 0.05; **p < 0.01; ***p < 0.001).

(B-H) Boxplot of risk scores and clinical correlation analysis (stage, T stage, N stage, M stage, gender, grade, and cluster).

Figure 8

m6A-related prognostic lncRNAs signature was related to the TME immune reaction.

(A-C) Scatterplot of correlation of risk score and immune cells, including M1 macrophages (A), M2 macrophages (B), and plasma cells (C).

(D-E) Boxplot of the relationship between risk score and the expression level of immune checkpoint genes, including HAVCR2 (D) and LAG3 (E).

(F-I) Boxplot of the relationship between risk score and drug sensitivity, including sunitinib (F), axitinib(G), sorafenib (H), rapamycin (I), pazopanib (J), temsirolimus (K), and gemcitabine (L).